Available online at www.sciencedirect.com
ScienceDirect
Polymer 49 (2008) 330–338
polymer
www.elsevier.com/locate/polymer

Role of multi-wall carbon nanotube network in composites to crystallization of isotactic polypropylene matrix

Donghua Xu, Zhigang Wang*

CAS Key Laboratory of Engineering Plastics, Joint Laboratory of Polymer Science and Materials, Beijing National Laboratory for Molecular Sciences, Institute of Chemistry, Chinese Academy of Sciences, Beijing 100080, PR China

Received 22 June 2007; received in revised form 5 November 2007; accepted 8 November 2007
Available online 22 November 2007

Abstract

The composites (iPP/CNTs) made of isotactic polypropylene (iPP) and multi-wall carbon nanotubes (CNTs) were prepared by solution blending. To improve compatibility between CNTs and iPP and to enhance dispersion of CNTs in iPP matrix, CNTs were chemically modified by grafting alkyl chains. The chemically modified CNTs had about 6 wt% grafted alkyl chains. Rheological measurements indicated that CNTs caused gelation in iPP/CNTs due to CNT network formation and the critical gelation CNT concentration was about 7.4 wt%, which was considered to be high due to the low CNT aspect ratio in this study. Crystallization behaviors of iPP/CNTs were studied by using optical microscopy (OM) and differential scanning calorimetry (DSC). Radial growth rates of spherulites during isothermal crystallization of iPP/CNTs with CNT concentrations less than 2.0 wt% measured by using OM showed decreasing trends with increasing CNT concentration. Avrami analysis of the exothermic heat flow curves during isothermal crystallization of iPP/CNTs measured by DSC indicated that crystallization rates were accelerated when CNT concentrations were lower than the critical gelation concentration, because CNTs mainly functioned as nucleating agents for crystallization, while crystallization rates did not change obviously when CNT concentrations were higher than the critical gelation concentration, because CNT network could form and mainly functioned to provide restriction to mobility and diffusion of iPP chains to crystal growth fronts.

Keywords: Isotactic polypropylene; Carbon nanotubes; Crystallization

1. Introduction

Isotactic polypropylene (iPP) is one of the most important commodity polymers. It is extensively used in industry to manufacture bottles, films, fibers, etc. However, the application of iPP has been limited by its tendency to brittleness at low temperatures. Therefore, a great deal of effort has been made to modify its mechanical properties such as blending iPP with inorganic fillers [1]. Several studies have been devoted to the uses of carbon nanotubes (CNTs) as fillers to improve performances of iPP or to achieve new properties of the composites, because of high aspect ratios, unusual mechanical and electronic properties of CNTs [2–4]. Because crystallization behavior would have a huge influence on mechanical properties of the filled iPP, several groups reported crystallization behaviors of iPP in the presence of CNTs [5–10]. Most of these studies focused on changes of iPP crystal forms [5,6] or nucleating ability of CNTs for iPP crystallization [7].

One recent study shows that combination of the extended shape, rigidity and deformability of CNTs allows CNTs to be well dispersed in polymer matrix in the form of disordered 'jammed' network structures at above a critical CNT concentration [2]. We predict that this CNT network can affect iPP crystallization in certain ways. Thus, iPP crystallization behaviors may be much different between those prior to and beyond CNT network formation. In fact, there have been several evidences in literatures to support this prediction. Haggenmueller et al. studied crystallization kinetics of polyethylene (PE) in the presence of single-wall carbon nanotube (SWNT) [11]. They found that addition of 1 wt% SWNT

* Corresponding author. Tel./fax: +86 10 62558172.
E-mail address: zgwang@iccas.ac.cn (Z. Wang).

0032-3861/$ - see front matter © 2007 Elsevier Ltd. All rights reserved.
doi:10.1016/j.polymer.2007.11.041

reduced the half crystallization time ($t_{1/2}$) to 7% of $t_{1/2}$ of neat PE at 122 °C, while additions from 1 wt% to 10 wt% SWNT provided only modest additional decreases of $t_{1/2}$. We consider that 10 wt% SWNT is sufficient for PE/SWNT to form gelation due to the SWNT network according to the SWNT aspect ratio in their study and the SWNT network may affect PE crystallization behaviors. Li et al. studied crystallization kinetics of poly(hexamethylene adipamide) (nylon 66) in the presence of multi-wall carbon nanotubes (CNTs) [12]. They observed that crystallization rate of nylon 66 during isothermal crystallization measured by DSC increased at first and then decreased with increasing CNT content. They suggested that the effect of CNTs on nylon 66 crystallization was twofold: CNTs provided heterogeneous nucleation sites for crystallization while CNT network hindered formation of large-size crystals. At low CNT contents, CNT surface initiated nylon 66 crystallization and the confinement effect was not significant. As the CNT content increased, although more CNTs could provide nucleation surface, the formed robust CNT network imposed a much more significant confinement effect on mobility of nylon 66 chains. This confinement effect overcame the nucleation effect and slowed down the overall crystallization kinetics [12]. Though the effects of CNT network on crystallization of semicrystalline polymers have been proposed, direct evidences are still missing. In the study reported here, we firstly determined the critical gelation CNT concentration for iPP/CNTs by using rheological methods, and then we further investigated the effects of CNT network on iPP crystallization behaviors in the composites.

2. Experimental section

2.1. Preparation and characterization of chemically modified multi-wall carbon nanotubes

To enhance dispersion of CNTs in iPP, commercially available multi-wall CNTs (produced by chemical vapor deposition (CVD) method, Shenzhen Nanotech Port Co., Ltd., China) were chemically modified as follows. CNTs were purified and converted into acid form [CNT(COOH)$_n$] *via* sonication in 1/3 relative volume ratio of nitric acid/sulfuric acid mixture at 40 °C. The resultant solid was washed with deionized water until the pH value was 6 and then an excessive NaOH solution was added until the pH value became 14, converting CNT(COOH)$_n$ into sodium salt form [CNT(COONa)$_n$]. The CNT(COONa)$_n$ nanotubes were recovered by centrifuging at 3000 rpm for 10 min, and then the resultant solid was washed with deionized water until the pH value was 6. Cetyltrimethylammonium bromide (CTAB), $C_{18}H_{37}Br$, CNT(COONa)$_n$ and water were mixed and the suspension was continuously refluxed under vigorous stirring for 12 h. When the stirring was stopped, the suspension separated to form a clear, colorless top solution with a black precipitate on the container bottom. The precipitate was collected and placed in a Soxhlet extractor. Deionized water (200 ml) was added to extract the remained CTAB over a period of 24 h, followed by addition of 200 ml chloroform to remove the remained $C_{18}H_{37}Br$ for another 24 h [13]. The solid material obtained from the Soxhlet extractor was dissolved in chloroform at 1 wt%. The solution was put in a sonication bath for 2 h and then was centrifuged at 3000 rpm for 10 min. The upper solution was collected and distilled to obtain the resultant solid material. Finally, the solid material, alkyl-modified CNTs, CNT$(COOC_{18}H_{37})_n$, was dried under vacuum at room temperature for further use. Thermogravimetric analysis (TGA) showed about 6 wt% grafted alkyl chains on CNT$(COOC_{18}H_{37})_n$ [13].

Structure and morphology of CNT$(COOC_{18}H_{37})_n$ were characterized by using scanning electron microscopy (SEM, Hitachi S-4300, made in Japan). A dilute solution of CNT$(COOC_{18}H_{37})_n$ in chloroform was dropped onto a clean aluminum foil to form a thin film after chloroform evaporated, and the thin film was subjected to SEM examination. Length distribution of CNT$(COOC_{18}H_{37})_n$ could be obtained from SEM images, which was used to obtain the average aspect ratio of CNT$(COOC_{18}H_{37})_n$.

2.2. Preparation of iPP/CNT composites

The iPP sample employed in this work was commercial product of the Aldrich Chemical Company. The iPP sample had mass average molecular weight, M_w, of 340,000 and number average molecular weight, M_n, of 97,000. iPP (3.4 g) was added into 110 ml xylene in a flask. The flask under protection of nitrogen atmosphere was put into an oil bath set at 130 °C. When iPP was dissolved for 20 min, the oil bath temperature was set to 120 °C. The iPP solution was continuously stirred for 1 h before CNT$(COOC_{18}H_{37})_n$ xylene suspension was added in. The CNT$(COOC_{18}H_{37})_n$ xylene suspension with CNT concentration of 0.25 wt% had been prepared with 2 h sonication. A certain amount of CNT$(COOC_{18}H_{37})_n$ xylene suspension was added into iPP solution to determine a suitable mass ratio of CNT$(COOC_{18}H_{37})_n$ to iPP. The mixture was continuously stirred for another 1.5 h. Then the mixture was deposited into a large quantity of methanol with a 1/7 volume ratio of the former to the latter. The precipitate of iPP/CNT$(COOC_{18}H_{37})_n$ composite was separated and washed with methanol for three times, and then was put in ventilation hood to let solvents evaporate for 48 h. The recovered composite was dried at 60 °C under vacuum for 3 days. By using the above procedure, eight samples were prepared, which possessed CNT$(COOC_{18}H_{37})_n$ concentrations of 0%, 0.2%, 0.5%, 1.0%, 2.0%, 3.8%, 7.4% and 9.1%, respectively. CNT$(COOC_{18}H_{37})_n$ and iPP/CNT$(COOC_{18}H_{37})_n$ composites are abbreviated as CNTs and iPP/CNTs, respectively, for simplicity in this article.

2.3. Determination of critical gelation CNT concentration for iPP/CNTs by rheology

Disk-shaped samples of iPP/CNTs with 1 mm thickness and 25 mm diameter for rheological measurements were prepared by hot-pressing at 200 °C using stainless steel die. A stress-controlled rheometer (AR2000, TA instrument Ltd.) was applied to measure dynamic rheological properties of

the samples at 200 °C. The measurements were performed under nitrogen atmosphere in an oscillatory shear mode using parallel-plate geometry (25 mm diameter) with 950 μm gap setting. The selected strain amplitude within a linear viscoelastic range was 2%. The samples were allowed to equilibrate for 10 min prior to frequency sweep. Sweeping frequencies covered a range from 100 rad/s to 0.1 rad/s.

2.4. Measurements of radial growth rates of spherulites in iPP/CNTs by using optical microscopy

An optical microscope (Carl Zeiss JENA, made in Germany) equipped with a CCD camera (HV1301UC, made by Daheng Company in Beijing, China) was used to study morphology and growth rates of spherulites of iPP/CNTs. Home-made dual-temperature microscope hot-stage was used to control temperature with temperature variations of ±0.1 °C. Film samples of iPP/CNTs with thicknesses of about 30 μm for optical microscopic observation were prepared by hot-pressing between cover glasses at 200 °C. For optical microscopic observation, the samples were first melted at 200 °C for 5 min to remove thermal histories, and then were rapidly transferred to different temperatures below the melting point of iPP for isothermal crystallization. The selected isothermal crystallization temperatures were between 136 °C and 144 °C. Note that for the samples with CNT concentrations above 1.0 wt%, they became too dark to be observed by using optical microscope due to strong light absorption.

2.5. Measurements of isothermal crystallization kinetics of iPP/CNTs by using DSC

A Perkin–Elmer DSC-7 differential scanning calorimeter was used to measure the overall isothermal crystallization kinetics of iPP/CNTs. The calorimeter was calibrated by using indium and zinc at a heating rate of 10 °C/min. Sample weights were about 5 mg. Aluminum pans were used. The samples were heated from 50 °C to 200 °C at a rate of 200 °C/min (the actual rate was about 197 °C/min) and held for 5 min to eliminate thermal histories, and then were quenched at a rate of 200 °C/min (the actual rate was about 82 °C/min) to desired isothermal crystallization temperatures. Heat flows during isothermal crystallization of iPP/CNTs at different temperatures were recorded. Crystallization kinetics of iPP/CNTs could be analyzed simply by using the Avrami equation [14] as follows:

$$\ln\left[-\ln\left(1-X_{(t)}\right)\right] = n\ln(t) + \ln(k) \quad (1)$$

where $X_{(t)}$ was the relative crystallinity, n was the Avrami exponent, k was the kinetic rate constant, and t was the crystallization time. Half crystallization time ($t_{1/2}$), which could represent the crystallization rate, was obtained by using the following equation:

$$t_{1/2} = [\ln(2/k)]^{1/n} \quad (2)$$

3. Results and discussion

Previous report shows that when CNT concentration in composites increases, carbon nanotube–polymer–carbon nanotube interactions begin to dominate and eventually lead to percolation and formation of an interconnected CNT network [15]. CNT network formation can be reflected by a gelation behavior of the composites from rheological viewpoint. The critical gelation CNT concentration directly relates to the CNT aspect ratio [16]. In order to estimate the CNT aspect ratio in this study, SEM images were collected. A typical SEM image of CNTs is shown in Fig. 1a. Length distribution of CNTs obtained from the image analysis is shown in Fig. 1b. The average length is about 564 nm. Since the diameters of CNTs in the range from 10 nm to 20 nm are reported by the producer, the average CNT aspect ratio in the range of 28–56 can be estimated. In Ref. [2], the CNT aspect ratio was in the range of 300–400, indicating that much longer CNTs had been used in that study, and accordingly, the gelation CNT concentration as low as about 1% volume fraction (2 wt%) was reported. While because CNTs used in this study have much lower aspect ratio, that is to say, much shorter CNTs have been used, and accordingly, a higher critical

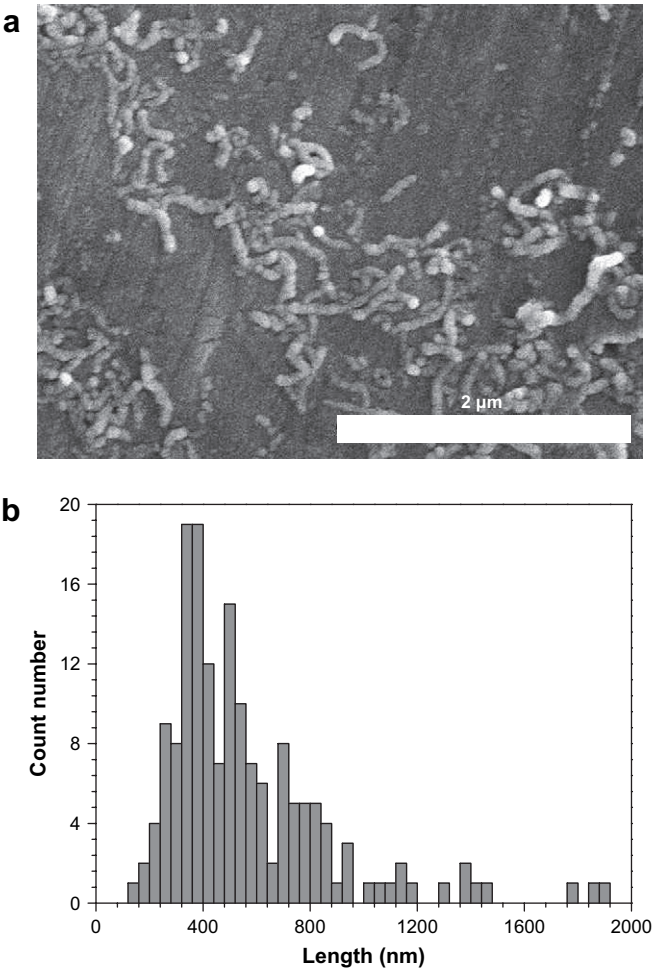

Fig. 1. SEM image of chemically modified CNTs, CNTs$(COOC_{18}H_{37})_n$ (a) and the corresponding length distribution of CNTs$(COOC_{18}H_{37})_n$ (b).

gelation CNT concentration would be expected for iPP/CNTs. The following rheological results can confirm this expectation.

Fig. 2a and b shows changes of storage modulus, G', and loss modulus, G'', of iPP/CNTs at different CNT concentrations with sweeping frequency, respectively. Note that the measuring temperature is 200 °C, which is above the melting point of iPP. At a fixed frequency, both G' and G'' increase with increasing CNT concentration. In addition, at a fixed CNT concentration, both G' and G'' increase with increasing frequency. Moreover, it can be found that G' seems to reach the plateaus at low frequencies for iPP/CNTs with CNT concentrations of 7.4 wt% and 9.1 wt%. This is indicative of a transition from liquid-like to solid-like viscoelastic behaviors. This non-terminal behavior at low frequencies for iPP/CNTs with high CNT concentrations can be attributed to the formed CNT network, which restrains long-range motions of polymer chains [17]. It also further infers that CNT network may restrain diffusion of polymer chains in the undercooled melt during crystallization, leading to changes of crystallization kinetics of polymer matrix. The network formation usually is accompanied by a gelation behavior. Frequency dependence of loss tangent (tan δ) can reflect more clearly about the appearance of gelation. It has been predicted that in the pre-gel regime, tan δ monotonically decreases with increasing frequency, which is a typical behavior for a viscoelastic liquid, while in the post-gel regime, a moderate increase of tan δ at low frequencies appears with increasing frequency, indicating a dominant elastic response in the composite [18]. Frequency dependence of tan δ for iPP/CNTs is shown in Fig. 2c. It can be found that for CNT concentrations of 7.4 wt% and 9.1 wt% moderate increases of tan δ at low frequencies do occur with increasing frequency, while for the lower CNT concentrations monotonic decreases of tan δ with increasing frequency are always observed. Therefore, the critical gelation CNT concentration for iPP/CNTs can be estimated to be around 7.4 wt%. The critical gelation CNT concentration of 7.4 wt% for iPP/CNTs in this study is much higher than that of 2 wt% in Ref. [2], which is considered to be induced by the lower CNT aspect ratio in this study than that in Ref. [2].

Pötschke et al. reported that temperature has a great influence on the critical gelation CNT concentration for polycarbonate/CNT (PC/CNT) composites [19]. The critical gelation CNT concentration for PC/CNTs changes from 5.0 wt% to 0.5 wt% with increasing temperature from 170 °C to 280 °C [19]. It has been explained in Ref. [19] that the temperature dependence may be associated with the combined carbon nanotube–polymer–carbon nanotube network rather than carbon nanotube–carbon nanotube network. Viscoelastic behavior of polymer chains may systematically change with temperature variation, resulting in change of the critical gelation CNT concentration. However, the carbon nanotube–carbon nanotube network may remain unchanged with temperature variation [19]. Referring to the report on PC/CNTs, it is thought that the critical gelation CNT concentration for iPP/CNTs at a crystallization temperature (for the undercooled melt) might be higher than that at 200 °C (for the melt), while the CNT network in iPP matrix for CNT concentration of 7.4 wt% may remain about the same when temperature decreases from 200 °C to the crystallization temperature, therefore, the effect of CNT network on iPP crystallization behaviors can still be studied, even though the exact gelation CNT concentration at

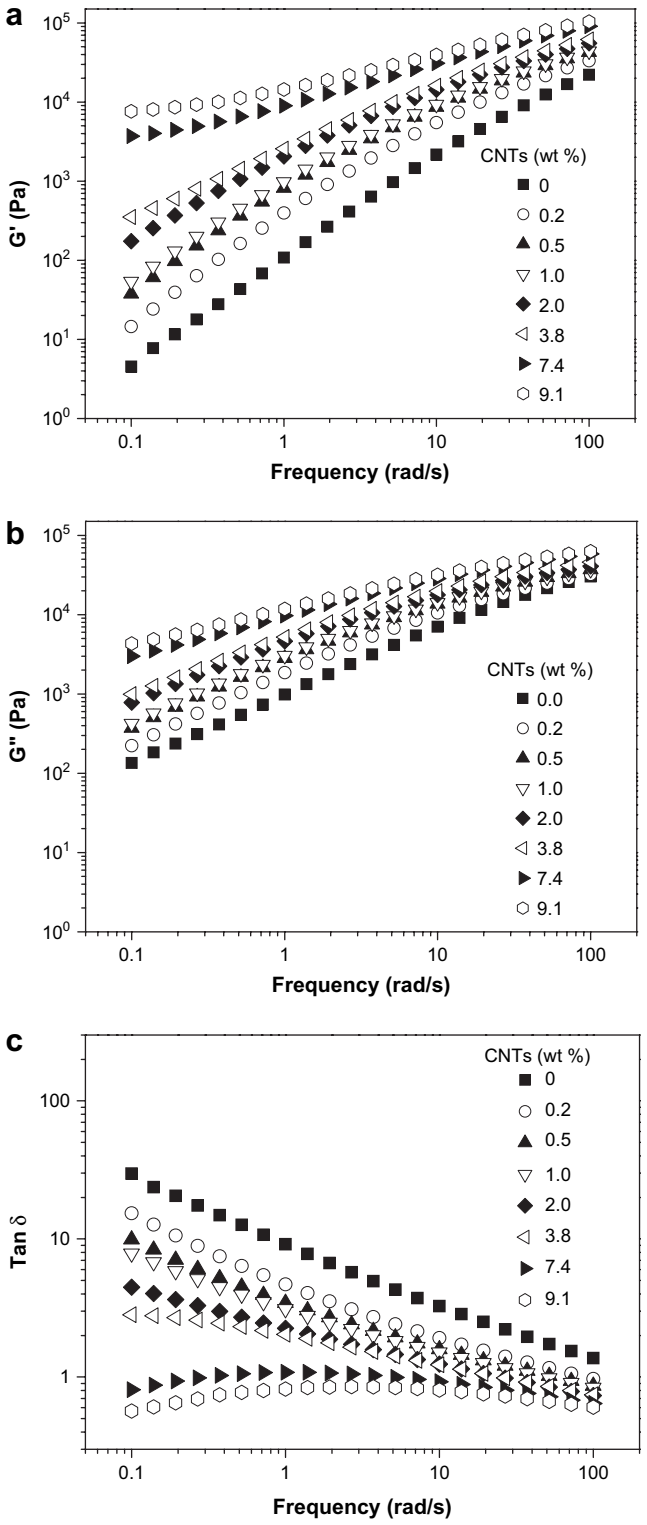

Fig. 2. Storage modulus (G') (a), loss modulus (G'') (b), and loss tangent, tan δ (c), as functions of frequency for iPP/CNTs with different CNT concentrations. Rheological measurements were performed with a strain of 2% at 200 °C.

the crystallization temperature cannot be precisely determined by rheological measurements.

Before crystallization behaviors of iPP/CNTs were investigated systematically, dispersion of CNTs in iPP matrix was evaluated by using optical microscopy. Optical micrograph of iPP/CNTs with CNT concentration of 1.0 wt% at 200 °C in bright field is shown in Fig. 3a. It can be seen that CNTs are relatively uniformly distributed in iPP matrix at a micrometer scale. Note that bright field was used because CNTs were black and iPP matrix itself alone was transparent in the molten state. Although there are still some sparse CNT aggregates, these aggregates just occupy a small CNT portion. Overall, CNTs are considered to reasonably 'well disperse' in iPP matrix in the current study, at least at the scales prescribed by our optical microscopic observation. The reasonably good dispersion is facilitated by interactions between iPP chains and grafted alkyl chains on CNT surface [13]. It should be pointed out that chemical modification on CNTs is quite necessary to enhance compatibility between CNTs and iPP and to improve CNT dispersion in iPP matrix, as can be easily confirmed by the relatively poor dispersion found when mixing pristine CNTs into iPP under equivalent conditions as blending the chemically modified CNTs (see Fig. 3b).

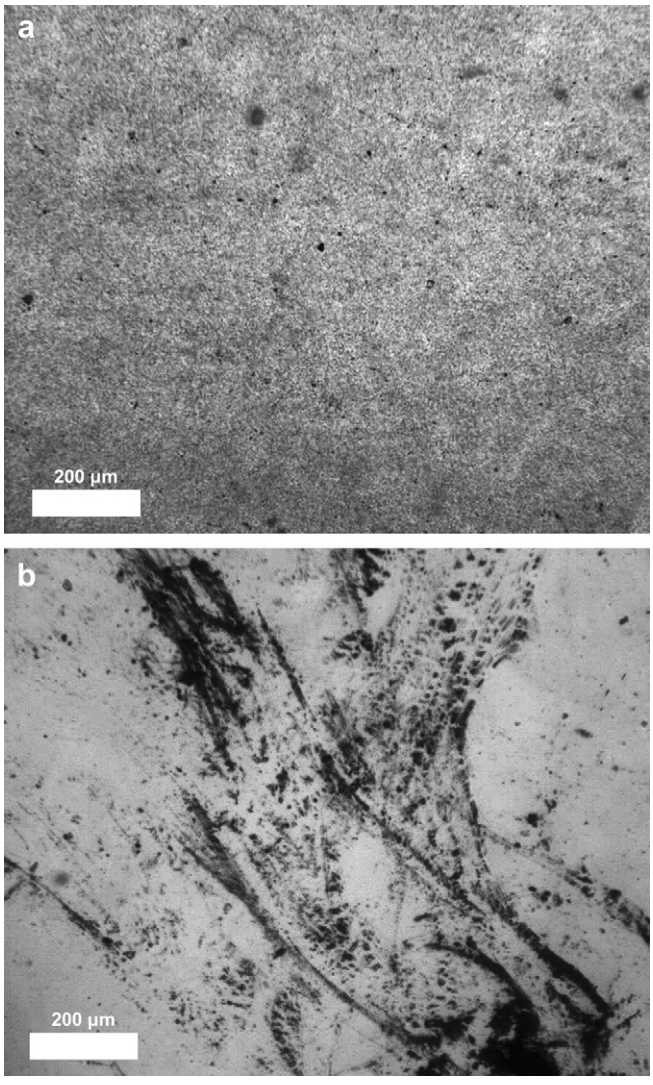

Fig. 3. Optical micrographs of iPP/CNTs($COOC_{18}H_{37}$)$_n$ (a) and iPP/pristine CNTs (b) with CNT concentration of 1.0 wt% at 200 °C in bright field.

Isothermal crystallization behaviors of iPP/CNTs with CNT concentrations less than 2.0 wt% at several selected temperatures between 136 °C and 144 °C were studied by using optical microscopy. When CNT concentrations were higher than 1.0 wt%, the samples became too dark to be well observed by using optical microscopy, for which crystallization kinetics was studied by using DSC. Typical optical micrographs taken during isothermal crystallization of iPP/CNTs with different CNT concentrations at 136 °C for certain times are presented in Fig. 4. It is obviously seen that the sizes of spherulites in neat iPP are much larger than that in iPP/CNTs with CNT concentration of 0.2 wt%. Nucleation density in the former is also obviously lower than that in the latter. Apparently, heterogeneous nucleation event is considered to occur mainly in the latter, due to nucleating effect of CNTs on primary crystallization of iPP [12,20,21]. Even though a lot of published papers discuss about the nucleation ability of CNTs on crystallization of semicrystalline polymers [12,20,21], the reasons why CNTs can be efficient nucleating agents have not been explained clearly. We consider that CNT surfaces might help decrease the energy barrier for nucleation of polymer crystallization. It is also found that the sizes of spherulites and nucleation density of iPP/CNTs show no obvious changes with increasing CNT concentration from 0.2 wt% to 1.0 wt%, which infers that the nucleating effect of CNTs may saturate at least at CNT concentration of 0.2 wt%. Here the word 'saturate' implies that a further elevation of CNT concentration does not further improve the nucleation effect [22,23]. The saturation essence of nucleation effect is worth further investigation. The radial growth rates (G) of spherulites in iPP/CNTs could be determined straightforward from time-resolved optical micrographs. Changes of G as functions of crystallization temperature for iPP/CNTs with different CNT concentrations are shown in Fig. 5. The G values decrease with increasing CNT concentration at each crystallization temperature, because viscosity of iPP/CNTs increases and accordingly, diffusion rate of iPP chains for crystal growth decreases with increasing CNT concentration. It is obvious that the energy barrier for transport of iPP chains in the undercooled melt increases with increasing CNT concentration [24]. At lower isothermal crystallization temperature, decreasing of G due to increasing CNT concentration is more significant, indicating more obvious effect of the energy barrier for transport of iPP chains on crystallization, while at higher isothermal crystallization temperature, decreasing of G due to increasing CNT concentration is less significant, indicating weakening effect of the energy barrier for transport of iPP chains on crystallization. Lower G values for iPP/CNTs at higher isothermal crystallization temperature are simply due to lower undercooling of the melt. It should be noted that we have not observed apparent immiscibility between CNTs and iPP and obvious migrations of CNTs between spherulites during crystallization of iPP/CNTs at the scales of our optical microscope. However, we do think that migrations of CNTs during crystallization at

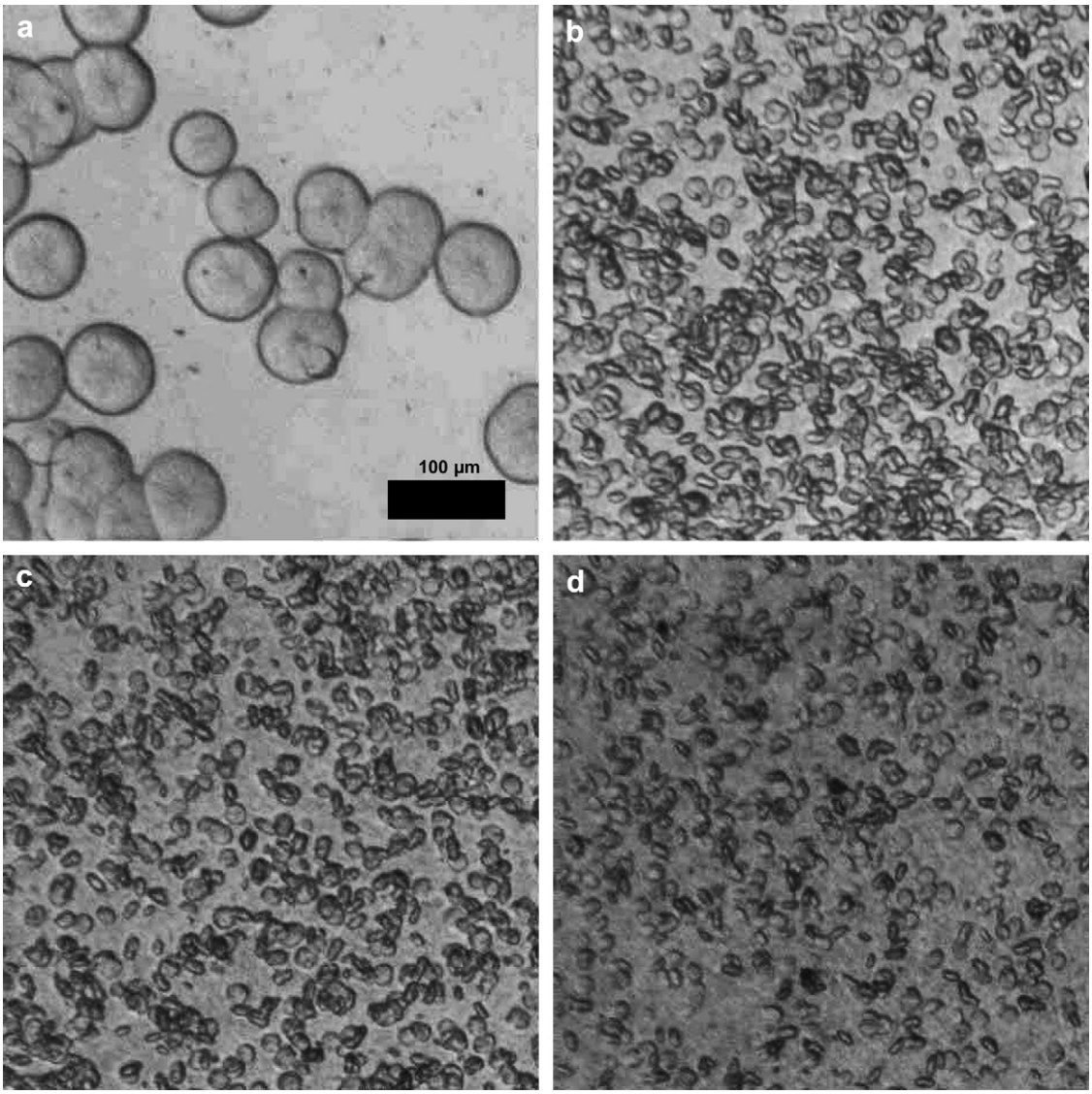

Fig. 4. Optical micrographs of iPP/CNTs with CNT concentrations of (a) 0 wt%, (b) 0.2 wt%, (c) 0.5 wt% and (d) 1.0 wt%, during isothermal crystallization at 136 °C for 21 min, 6 min, 6 min, and 6 min, respectively. Optical micrographs were taken in bright field.

smaller scales might truly take place since it is well known that for semicrystalline polymer/inorganic particle systems the inorganic particles usually segregate to crystal growth fronts. CNTs are expected to be excluded from iPP crystals during crystallization, resulting in aggregations of CNTs in the gaps between spherulites or into the amorphous region of lamellar stacks, or at the boundaries of lamellar stacks. The exact locations of CNTs in the final crystal morphology are worth further investigation.

DSC measurements have been performed to study crystallization kinetics of iPP/CNTs with various CNT concentrations, including the ones that cannot be studied by using optical microscopy. Fig. 6 shows exothermic heat flow curves of iPP/CNTs during isothermal crystallization at 134 °C. It can be seen from Fig. 6 that peak position of the exothermic heat flow curve (standing for the time when the maximum crystallization rate appears, t_{max}) shifts to a much shorter time region when only adding 0.2 wt% CNTs, indicating an obviously enhanced overall crystallization rate due to the nucleating effect of CNTs. A more interesting finding is as follows. For iPP/CNTs with CNT concentrations less than 7.4 wt%, which is the estimated critical gelation CNT concentration for iPP/CNTs, t_{max} decreases with increasing CNT concentration; while for iPP/CNTs with CNT concentrations equal to and higher than 7.4 wt%, t_{max} does not show further obvious decrease compared with that of iPP/CNTs with CNT concentration of 3.8 wt%; nevertheless, t_{max} of iPP/CNTs with CNT concentration of 7.4 wt% is even slightly higher than that of iPP/CNTs with CNT concentration of 3.8 wt%. The above results indicate that crystallization rate of iPP/CNTs increases with increasing CNT concentration below the critical gelation CNT concentration, but keeps about constant above the critical gelation CNT concentration. It should be noted that multiple crystallization cycles (repeated melt crystallization/heating/melt crystallization cycles) do not affect much on the overall crystallization behaviors of iPP/CNTs, indicating the structural

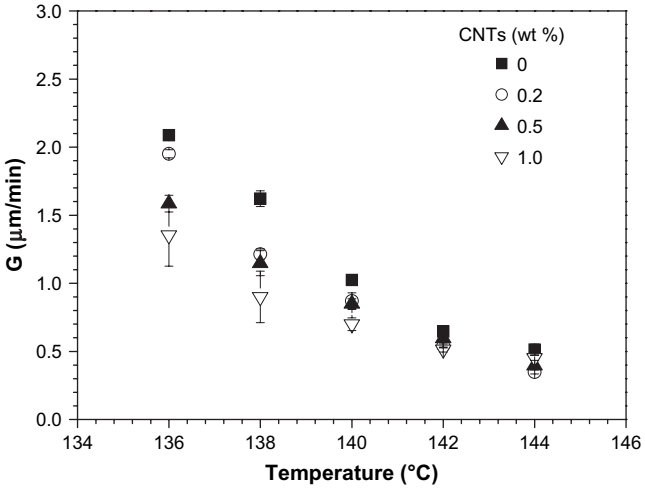

Fig. 5. Changes of radial growth rate of spherulites, G, as functions of crystallization temperature for iPP/CNTs with CNT concentrations of 0 wt%, 0.2 wt%, 0.5 wt% and 1.0 wt%.

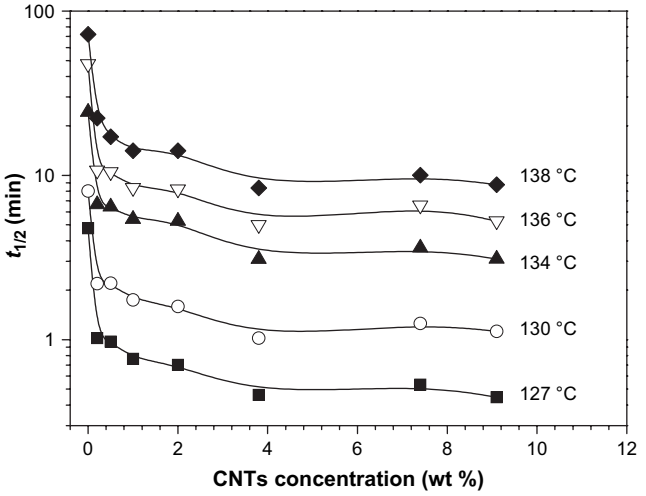

Fig. 7. Changes of half crystallization time, $t_{1/2}$, of iPP/CNTs with CNT concentration at crystallization temperatures of 127 °C, 130 °C, 134 °C, 136 °C and 138 °C.

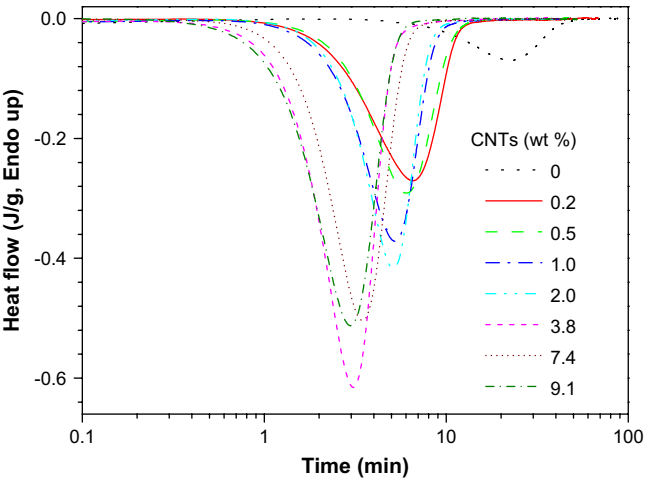

Fig. 6. Heat flow curves of iPP/CNTs with different CNT concentrations during isothermal crystallization at 134 °C.

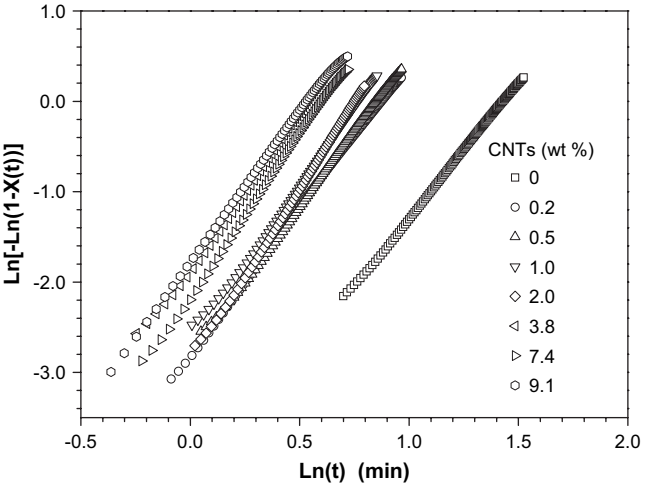

Fig. 8. Avrami plots for iPP/CNTs with different CNT concentrations during isothermal crystallization at 134 °C.

thermal stability of iPP/CNTs. However, we did observe very slight increases in t_{max} with the cycle number, but the increases are not significant. The slight increases in t_{max} and the corresponding decreases in isothermal crystallization rate with increasing cycle number can be contributed to aggregation of CNTs, which surely decreases nucleation density and crystallization rate. Nevertheless, we report DSC data of the samples which do not experience multiple crystallization cycles in this article, thus the data are comparable.

To quantitatively compare crystallization kinetics of iPP/CNTs with different CNT concentrations, the Avrami analyses on DSC data have been conducted and the half crystallization time, $t_{1/2}$, can be obtained. Changes of $t_{1/2}$ of iPP/CNTs with increasing CNT concentration at different crystallization temperatures are shown in Fig. 7. An obviously observable phenomenon is about an initially rapid decrease of $t_{1/2}$ and subsequently modest decrease of $t_{1/2}$, followed by about constant $t_{1/2}$, with increasing CNT concentration at each isothermal crystallization temperature. For example, at 127 °C, addition of 0.2 wt% CNTs reduces $t_{1/2}$ to 21% of $t_{1/2}$ of neat iPP, additions of 0.2–3.8 wt% CNTs only reduce $t_{1/2}$ from 21% to 10% of $t_{1/2}$ of neat iPP, and additions of above 3.8 wt% CNTs maintain about constant 10% of $t_{1/2}$ of neat iPP.

Plots of $\ln[-\ln(1-X(t))]$ versus $\ln(t)$ for iPP/CNTs isothermally crystallized at 134 °C are shown in Fig. 8, in which the curves show linear relationships and the Avrami exponents (n) can be obtained from the slopes in the plots of $\ln[-\ln(1-X(t))]$ versus $\ln(t)$. Changes of the Avrami exponent with increasing CNT concentration for iPP/CNTs crystallized at different temperatures are shown in Fig. 9. The Avrami exponent values are around 3 and do not change obviously with increasing CNT concentration. This result is consistent with the crystal morphology shown in Fig. 4. It implies that three-dimensional crystal growths happen for the iPP spherulites in the composites. Previous reports on crystallization kinetics of iPP/CNTs showed that the Avrami exponent was practically

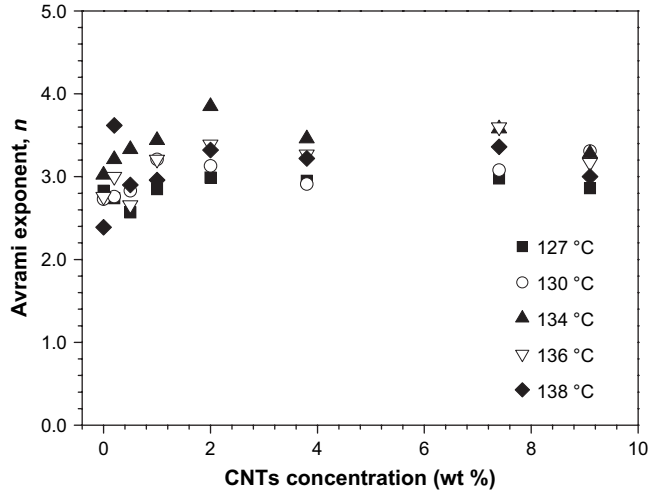

Fig. 9. Changes of the Avrami exponent (n) of iPP/CNTs with CNT concentration at different isothermal crystallization temperatures.

unchanged with the addition of CNTs, when iPP/CNTs crystallized isothermally at high temperature [6,9]. Some other works showed that the Avrami exponent of iPP/CNTs was lower than that of neat iPP, when iPP/CNTs crystallized non-isothermally [7]. Different Avrami exponent values during crystallization of iPP/CNTs in literatures may be related to different experimental conditions.

The degree of crystallinity (X_c) denoting crystallinity of iPP itself in iPP/CNTs during isothermal crystallization can be obtained from exothermic enthalpy (ΔH_c) of the heat flow curve by using $X_c = \Delta H_c/[(1-\varphi)\Delta H_m)]$, where ΔH_m is heat fusion of iPP with 100% crystallinity (209 J/g) [25] and φ is CNT mass fraction in iPP/CNTs. Changes in X_c of iPP in iPP/CNTs with increasing CNT concentration at different temperatures are shown in Fig. 10. It can be seen that the X_c values do not show obvious changes with increasing CNT concentration. The results are consistent with those in Refs. [8,9].

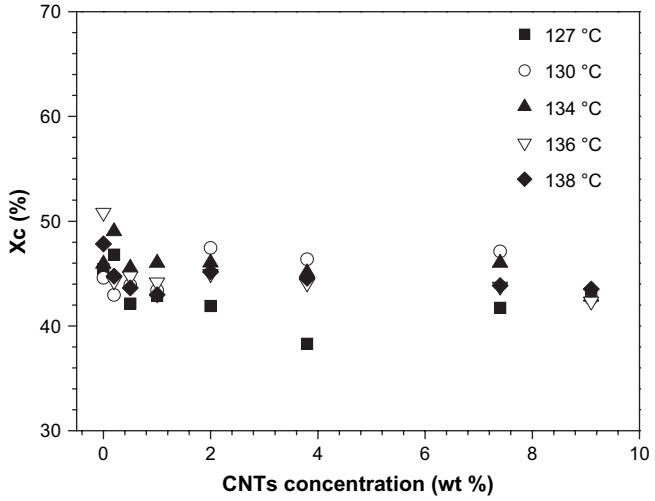

Fig. 10. Changes in crystallinity (X_c) of iPP/CNTs with CNT concentration at different isothermal crystallization temperatures.

It has been considered that the addition of CNTs could have two types of effects on crystallization behaviors of iPP in iPP/CNTs. On one hand, CNTs may function as heterogeneous nucleating agents for iPP crystallization; on the other hand, CNTs may hinder mobility and diffusion of iPP chains in the undercooled melt for crystallization. The nucleating effect of CNTs in iPP/CNTs can be found by using optical microscopy (see Fig. 4). Decreases in mobility and diffusion of iPP chains can be confirmed by decreases of radial growth rates of iPP spherulites with increasing CNT concentration (see Fig. 5). With further increasing CNT concentration, CNT network can form and it further restrains diffusion of iPP chains, which can be confirmed by non-terminal behavior at low frequencies in rheological measurements (see Fig. 2a). Below the critical gelation CNT concentration, nucleating effect of CNTs is dominant and diffusion of iPP chains is not obviously restricted, thus, the half crystallization time, $t_{1/2}$, decreases with increasing CNT concentration (see Fig. 7). While above the critical gelation CNT concentration, nucleating effect of CNTs almost saturates, but restriction of CNT network to diffusion of iPP chains to crystal growth fronts becomes dominant, thus, $t_{1/2}$ keeps about constant.

It is worth mentioning that for polymer nanocomposites containing clays, the accelerated crystallization at low clay concentrations and retardation to crystallization at high clay concentrations have also been reported [26–28]. It is basically agreed that clay particles can serve as additional nucleation sites for crystallization and this can increase crystallization rate at low clay concentrations. However, different mechanisms have been postulated about how crystallization rate is retarded at high clay concentrations. One mechanism postulates that clays act as non-crystallizable barriers for polymer crystallization [26]. At high clay concentrations, non-crystallizable barriers disturb crystal growth by forcing the growing lamellar stacks along a more tortuous growth path and can possibly even stop several from growing [26]. Another proposed mechanism is that diffusion of polymer chains to growing crystallites is hindered at high clay concentrations [27]. In fact, these two mechanisms may act at the same time during crystallization. According to the results about retardation of crystallization rate at high concentrations of CNTs and clays [11,12,26–28], we suggest that further investigation on this phenomenon in other polymer/nanofiller composites is necessary.

4. Conclusions

Isotactic polypropylene (iPP) and multi-wall carbon nanotubes (CNTs) were solution blended to prepare the composites, iPP/CNTs. CNTs were chemically modified by grafting alkyl chains to improve compatibility between CNTs and iPP and to enhance dispersion of CNTs in iPP matrix. CNTs could cause gelation of iPP/CNTs at the critical CNT concentration of 7.4 wt% due to CNT network formation from rheological measurements. The high critical gelation CNT concentration of 7.4 wt% for iPP/CNTs was due to the low CNT aspect ratio in this study. Optical microscopic

observation showed a decreasing trend with increasing CNT concentration for radial growth rates of spherulites of iPP/CNTs with CNT concentrations less than 2.0 wt% during isothermal crystallization. Avrami analysis to isothermal crystallization data from DSC measurements indicated that crystallization rates were accelerated when CNT concentrations were less than the critical gelation CNT concentration, because CNTs mainly functioned as the nucleating agents for crystallization; while crystallization rates did not change obviously when CNT concentrations were higher than the critical gelation CNT concentration, because CNT network formed and mainly provided restriction to mobility and diffusion of iPP chains for crystallization.

Acknowledgments

Z.G. Wang thanks financial supports from ''One Hundred Young Talents'' Program of Chinese Academy of Sciences, National Science Foundation of China with grant number 10590355 for the Key Project on Evolution of Structure and Morphology during Polymer Processing and National Science Foundation of China with grant number 20674092.

References

[1] Thio YS, Argon AS, Cohen RE, Weinberg M. Polymer 2002;43:3661–74.
[2] Kharchenko SB, Douglas JF, Obrzut J, Grulke EA, Migler KB. Nat Mater 2004;3:564–8.
[3] Kashiwagi T, Grulke E, Hilding J, Groth K, Harris R, Butler K, et al. Polymer 2004;45:4227–39.
[4] Chang TE, Jensen LR, Kisliuk A, Pipes RB, Pyrz R, Sokolov AP. Polymer 2005;46:439–44.
[5] Grady BP, Pompeo F, Shambaugh RL, Resasco DE. J Phys Chem B 2002;106:5852–8.
[6] Bhattacharyya AR, Sreekumar TV, Liu T, Kumar S, Ericson LM, Hauge RH, et al. Polymer 2003;44:2373–7.
[7] Assouline E, Lustiger A, Barber AH, Cooper CA, Klein E, Wachtel E, et al. J Polym Sci Part B Polym Phys 2003;41:520–7.
[8] Valentini L, Biagiotti J, Kenny JM, Santucci S. Compos Sci Technol 2003;63:1149–53.
[9] Seo MK, Lee JR, Park S. J Mater Sci Eng A 2005;404:79–84.
[10] Leelapornpisit W, Ton-That M, Perrin-Sarazin F, Cole KC, Denault J, Simard B. J Polym Sci Part B Polym Phys 2005;43:2445–53.
[11] Haggenmueller R, Fischer JE, Winey KI. Macromolecules 2006;39:2964–71.
[12] Li LY, Li CY, Ni CY, Rong LX, Hsiao B. Polymer 2007;48:3452–60.
[13] Xu DH, Liu H, Yang L, Wang ZG. Carbon 2006;44:3226–31.
[14] Wunderlich B. Macromolecular physics, vol. 2. New York: Academic Press; 1976. p. 132–8.
[15] Pötschke P, Fornes TD, Paul DR. Polymer 2002;43:3247–55.
[16] Garboczi EJ, Snyder KA, Douglas JF, Thorpe MF. Phys Rev E 1995;52:819–28.
[17] Du F, Scogna RC, Zhou W, Brand S, Fischer JE, Winey KI. Macromolecules 2004;37:9048–55.
[18] Liu CY, Zhang J, He JS, Hu GH. Polymer 2003;44:7529–32.
[19] Pötschke P, Abdel-Goad M, Alig I, Dudkin S, Lellinger D. Polymer 2004;45:8863–70.
[20] Anand KA, Agarwal US, Joseph R. Polymer 2006;47:3976–80.
[21] Kim JY, Park HS, Kim SH. Polymer 2006;47:1379–89.
[22] Sabino MA, Ronca G, Müller AJ. J Mater Sci 2000;35:5071–84.
[23] Zhou ZX, Wang XL, Wang YZ, Yang KK, Chen SC, Wu G, et al. Polym Int 2006;55:383–90.
[24] Avella M, Cosco S, Volpe GD, Errico ME. Adv Polym Technol 2005;24:132–44.
[25] Martuscelli R, Silvestre C, Abate G. Polymer 1982;23:229–37.
[26] Homminga D, Goderis B, Dolbnya I, Reynaers H, Groeninckx G. Polymer 2005;46:11359–65.
[27] Fornes TD, Paul DR. Polymer 2003;44:3945–61.
[28] Jimenez G, Ogata N, Kawai H, Ogihara T. J Appl Polym Sci 1997;64:2211–20.